



Response of stratospheric water vapour to CO₂ doubling in WACCM

Tongmei Wang^{1,2} · Qiong Zhang² · Maartje Kuilman¹ · Abdel Hannachi¹

Received: 31 October 2019 / Accepted: 23 April 2020 / Published online: 30 April 2020
© The Author(s) 2020

Abstract

Stratospheric water vapour (SWV), as a greenhouse gas, modulates the radiative energy budget of the climate system. It is sensitive to, and plays a significant role in the climate change. In this study, we investigate the SWV response to CO₂ increase with the Whole Atmosphere Community Climate Model (WACCM). In addition, we study its possible feedback on stratospheric temperature and relevant mechanisms. In our model experiments, the CO₂ concentration and sea surface temperature (SSTs) are changed at the same time, as well as separately, to enable separating the radiative-photochemical and dynamical response to CO₂ doubling scenarios. The model results show that the response of SWV to CO₂ doubling is dominated by the changes in the SSTs, with an increase of the SWV concentration by ~6 to 10% in most of the stratosphere and more than 10% in the lower stratosphere, except for winter pole in the lower stratosphere, where the CO₂ doubling decreases water vapour. The increase of SWV is mostly due to a dynamical response to the warm SSTs. Doubled CO₂ induces warm SSTs globally and further leads to moist troposphere and a warmer tropical and subtropical tropopause, resulting in more water vapour entering stratosphere from below. As a greenhouse gas, large increase of SWV in the lower stratosphere, in turn, affects the stratospheric temperature, resulting in a warming of the tropical and subtropical lower stratosphere, offsetting the cooling caused by CO₂ doubling.

Keywords Stratospheric water vapour · Response · CO₂ doubling

1 Introduction

Human activities have caused a significant increase in the concentration of greenhouse gases. The annual rate of increase in atmospheric carbon dioxide (CO₂) over the past 60 years is about 100 times faster than in previous natural increases, such as those that occurred at the end of the last ice age 11,000–17,000 years ago. The amount of CO₂ is expected to double before the end of the twenty-first century (Brasseur and Hitchman 1988). The increase of CO₂ leads to an increase in the Earth's surface and tropospheric temperatures. However, the increased CO₂ actually cools the middle atmosphere. This is due to a decrease in atmospheric density with altitude: the infrared bands that enable trace gases to absorb and emit radiation become more optically

thin, and radiative cooling begins to dominate (Manabe and Strickler 1964; Manabe and Wetherald 1975; Fels et al. 1980; Gillett et al. 2003). Subsequent model simulations of the stratosphere-mesosphere (e.g., Fomichev et al. 2007; Garcia et al. 2007; Lübken et al. 2013) clarified that while CO₂ is the dominant driver of temperature change in the atmosphere, methane (CH₄) and ozone (O₃), and possibly also water vapour play significant roles in the stratosphere and mesosphere.

Stratospheric water vapour (SWV) modulates the radiative energy budget of the climate system as a greenhouse gas (Forster and Shine 2002). The observed increases in SWV were suggested to lead to a stratospheric cooling of similar magnitude to that by stratospheric O₃ losses (Forster and Shine 1999; Smith et al. 2001), and this increase potentially feeds back to and amplifies global warming (Dessler et al. 2013; Huang et al. 2016). Even though the exact importance of the feedback remains controversial, it is increasingly recognized that SWV is projected to increase with global warming in the simulations of general circulation models (Gettman et al. 2010). Radiative forcing associated with SWV changes has been quantified using different radiation kernels

✉ Tongmei Wang
tongmei.wang@misu.su.se

¹ Department of Meteorology, Stockholm University, Stockholm, Sweden

² Department of Physical Geography, Stockholm University, Stockholm, Sweden

(e.g. Forster et al. 2001). Solomon et al. (2010) examined the dependence of surface radiative forcing on the vertical distribution of SWV, illustrating that water vapour near the tropopause exerts the largest radiative forcing on the surface. Gilford et al. (2016) estimated that the lower SWV concentrations in the period of 2005–2013, compared to the 1990s, result in a difference in radiative forcing between the two periods of about -0.045 W m^{-2} . This would produce about 12% as large as, but of opposite sign to the concurrent greenhouse gas warming by CO_2 . Sensitivity of estimated radiative forcing to the representation of SWV in radiation codes has been discussed (Forster et al. 2001), and differences of up to 96% in SWV adjusted radiative forcing between different radiative codes were reported by a comparative study (Maycock and Shine 2012). The radiative impacts of SWV variations have been assessed using different models with varying degrees of sophistication. Maycock et al. (2013) simulated the atmospheric response to idealized changes in SWV using a vertically extended atmosphere model and concluded that the long-term increase in SWV may cool the stratospheric temperature, enhance the Brewer–Dobson circulation (BDC), and might even induce a poleward shift of storm tracks.

Water vapour and temperature are strongly coupled in the stratosphere (Dessler et al. 2013), therefore a complete understanding of stratospheric climate change requires accounting for the influence of changing water vapour concentrations. However, observed long-term changes in SWV remain a puzzle (Randel et al. 2004; Hurst et al. 2011; Fueglistaler 2012), since the processes that are expected to control SWV such as methane oxidation and tropical tropopause temperatures do not show long-term behaviour consistent with the derived water vapour trends. The exact mechanism of SWV change due to the climate warming is still an important unknown in the present discussion of climate change and needs further investigation. The primary objective of this study is to investigate the mechanisms of response of SWV and temperature to a doubling of the CO_2 -concentration with respect to the pre-industrial (PI) conditions.

With respect to the increasing CO_2 -concentration, two aspects of the stratospheric response are considered separately: (i) the radiative photochemical response in nature driven by the CO_2 -induced cooling, which is intrinsic response, and (ii) the dynamical response to the change in tropospheric climate driven by the upward propagating waves and their induced circulation. The radiative response should be robust, while the dynamical response can be more model-dependent. Rind et al. (2002) investigated CO_2 doubling effects under two different sea surface conditions and pointed out that the SST distribution is very important for the stratospheric response to doubled CO_2 . Sigmond et al. (2004) separated the tropospheric and stratospheric effects

by CO_2 doubling in the troposphere and stratosphere separately, as well as CO_2 doubling in both. It was found that the combined response was equal to the sum of the separate responses, confirming that the two aspects of the response are distinct. Schmidt et al. (2006) separated radiative-photochemical and dynamical effects by controlling the SSTs, as if only change the SSTs, then the stratospheric response to CO_2 is driven only by dynamical effects from the troposphere alone. In this paper we separate the two aspects of the response by changing the CO_2 concentration and SSTs combined or separated. The climate sensitivity experiments are performed by the Whole Atmosphere Community Climate Model (WACCM), which is a high-top global climate system model, including the full middle atmosphere chemistry.

Following the description of the model and the experimental setup in Sect. 2, the response of SWV to doubled CO_2 in the atmosphere and/or warm SSTs are given by comparing the results from different experiments in Sect. 3. The response of the residual circulation related to SWV transport are given in Sect. 4. In Sect. 5, the temperature changes and SWV feedback to temperature in the stratosphere are described. The response of SWV to warm SSTs, obtained from an equilibrium simulation to CO_2 doubling are discussed in Sect. 6. Conclusions are given in the last section.

2 Model description and experimental setup

With interactive chemistry along with an extension to the thermosphere, WACCM has been used extensively to study stratospheric dynamics. WACCM is a “high top” atmosphere model based on the NCAR Community Climate System Model (CESM) that extends in altitude from the surface to the lower thermosphere (5.1×10^{-6} hPa, approximately 140 km). WACCM includes all of the physical parameterizations of the Community Atmospheric Model version 4 (CAM4), as well as fully interactive chemistry (Neale et al. 2013; Marsh et al. 2013). It consists of 66 vertical levels and horizontal resolution of 1.9° latitude by 2.5° longitude. The model includes an updated parameterization of non-orographic gravity waves generated by frontal systems and convection and a surface stress due to unresolved topography (Garcia et al. 2007; Richter et al. 2010). The surface stress led to a big improvement in the frequency of the Northern Hemisphere sudden stratospheric warmings (SSWs) in uncoupled simulations (Richter et al. 2010). The model’s chemistry module is based on the Model for Ozone and Related Chemical Tracers, version 3 (MOZART-3), which was designed to represent the chemical and physical processes from the troposphere through the lower mesosphere (Kinnison et al. 2007).

In this study, first we perform a control experiment (CTL) under PI conditions, forced by PI sea surface temperature (SST) and sea ice (referred to SSTs from now on). The PI CO₂-concentration is 280 ppm, and the SSTs are from the CMIP5 PI control simulation by the fully coupled earth system model CESM (Hurrell et al. 2013). We run sensitivity experiments by doubling the CO₂-concentration from PI level to 560 ppm. In this case, the surface level CO₂ mixing ratio is doubled in the model, and elsewhere in the atmosphere is calculated according to WACCM's chemical model.

A CO₂ doubling combined experiment, under equilibrium condition, is forced by doubling the CO₂-concentration and warm SSTs (CT1). The warm SSTs used here are produced by a coupled CESM simulation driven by CO₂ doubling (Wen et al. 2018). The increase in CO₂ leads to a decrease in the Arctic sea ice. Sea ice melting provides freshwater to the ocean, which weakens the deep-water formation in the North Atlantic and the Atlantic meridional overturning circulation (AMOC) (Jahn and Holland 2013; Thornalley et al. 2018). The reduced AMOC results in cooling of the subpolar Atlantic, known as the “warming hole” (Sevellec et al. 2017; Caesar et al. 2018). The change in the AMOC is of great interest to the climate research community (Kim and An 2013; Drijfhout et al. 2012). Wen et al. (2018) run the coupled CESM in CO₂ doubling scenarios for 2000 years and they found a reduced AMOC reaching an equilibrium stage in the first 500 years, which is consistent with other modelling results. We take SSTs from their first equilibrium stage as the warm SSTs (wSST in tables and figures). The SST anomalies from PI condition (Fig. 1) show warming everywhere except a small region in the North Atlantic, which is known as the “warming hole”.

To explore the response of SWV to the change in CO₂ and SSTs separately, two more sensitivity experiments are performed: one is doubled CO₂ experiment without SSTs

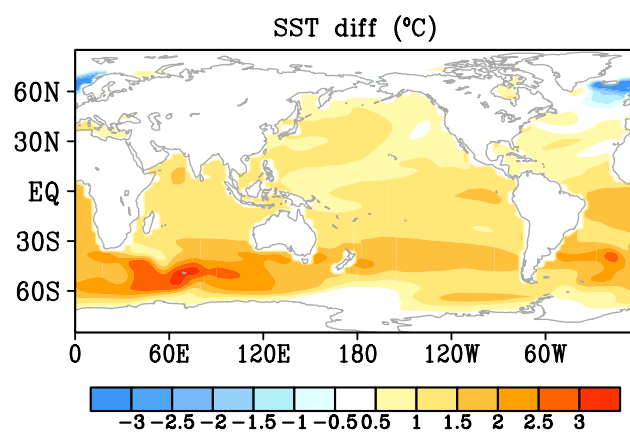


Fig. 1 Annual mean change in sea surface temperature in warm SSTs induced by CO₂ doubling in the coupled CESM compared to the PI SSTs

change from PI (C1), another one is warm SSTs without CO₂ doubling in the atmosphere (T1). See Table 1. All experiments are run for 50 years, the last 40 years are used for the analysis.

The climatology of the seasonal mean SWV and temperature in CTL run are shown in Fig. 2. The figure compares well with SWV from satellite observation (Wang et al. 2018). This shows that under the PI conditions, WACCM captures the main features of SWV and temperature seasonal mean climatology, suggesting that stratospheric processes are well represented in WACCM.

3 Response of SWV to doubled CO₂ and/or warm SSTs

The response of SWV to CO₂ doubling is separated into the response induced by doubled CO₂ alone and the response produced by changes in the SSTs. Figure 3 shows the relative changes in SWV percentage produced by the CO₂ doubling for the different experimental setups. The simulated changes are statistically significant, at the 5% level, throughout most of the stratosphere. With the doubled CO₂ only (C1), there is a decrease in SWV by ~2 to 6% in most of the stratosphere and more than 10% in the two polar regions of the lower stratosphere, Fig. 3b, e. The warm SSTs run (T1) shows an increase in SWV by ~6 to 10% in most of the stratosphere, and more than 10% in the lower stratosphere, especially in the tropics (Fig. 3c, f). The response of SST is dynamical by definition, which can only be done through wave propagation from the troposphere to the stratosphere (Holton et al. 1995). The SWV response of the combined CO₂ doubling and warm SSTs (Fig. 3a, d) is approximately equal to the sum of the two responses in C1 and T1. This is consistent with the results of Fomichev et al. (2007) who showed, based on the Canadian Middle Atmosphere Model (CMAM), that the radiative-photochemical response to the doubled CO₂ alone and the changes in SSTs are additive in most of the stratosphere. This means that the CO₂ doubling influences the SWV in two ways namely, (i) radiatively through in situ changes associated with changes in CO₂ or (ii) dynamically through changes in stratospheric wave forcing. In

Table 1 Setup of the model experiments

Experiment	Name	CO ₂ concentration (ppm)	SSTs
Pre-industrial (PI)	CTL	280	PI SSTs
Doubled CO ₂ and wSST	CT1	560	wSST
Doubled CO ₂	C1	560	PI SSTs
Warm SSTs	T1	280	wSST

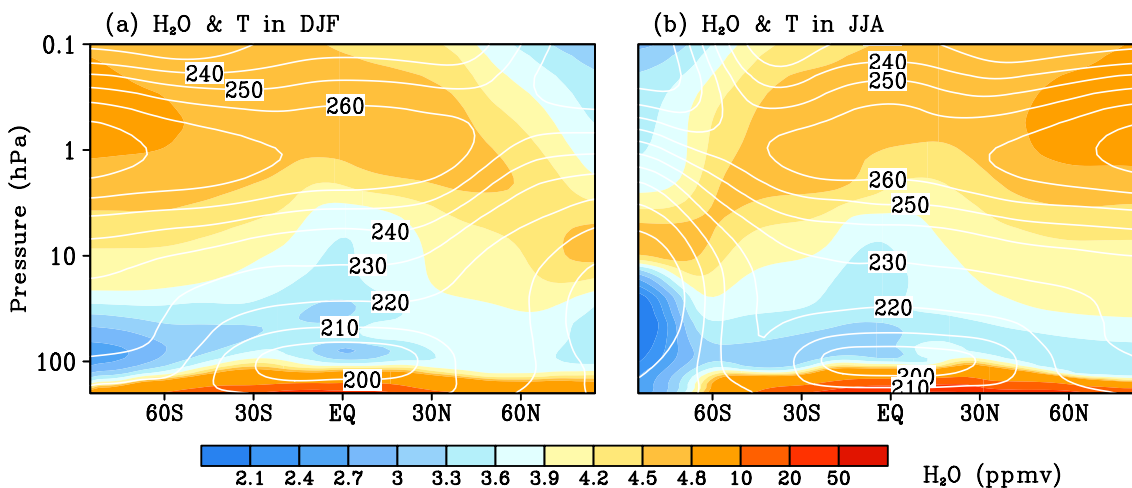


Fig. 2 The climatological seasonal mean SWV (shading) and temperature (contours) distribution from the CTL (PI) run for DJF means (a) and JJA means (b)

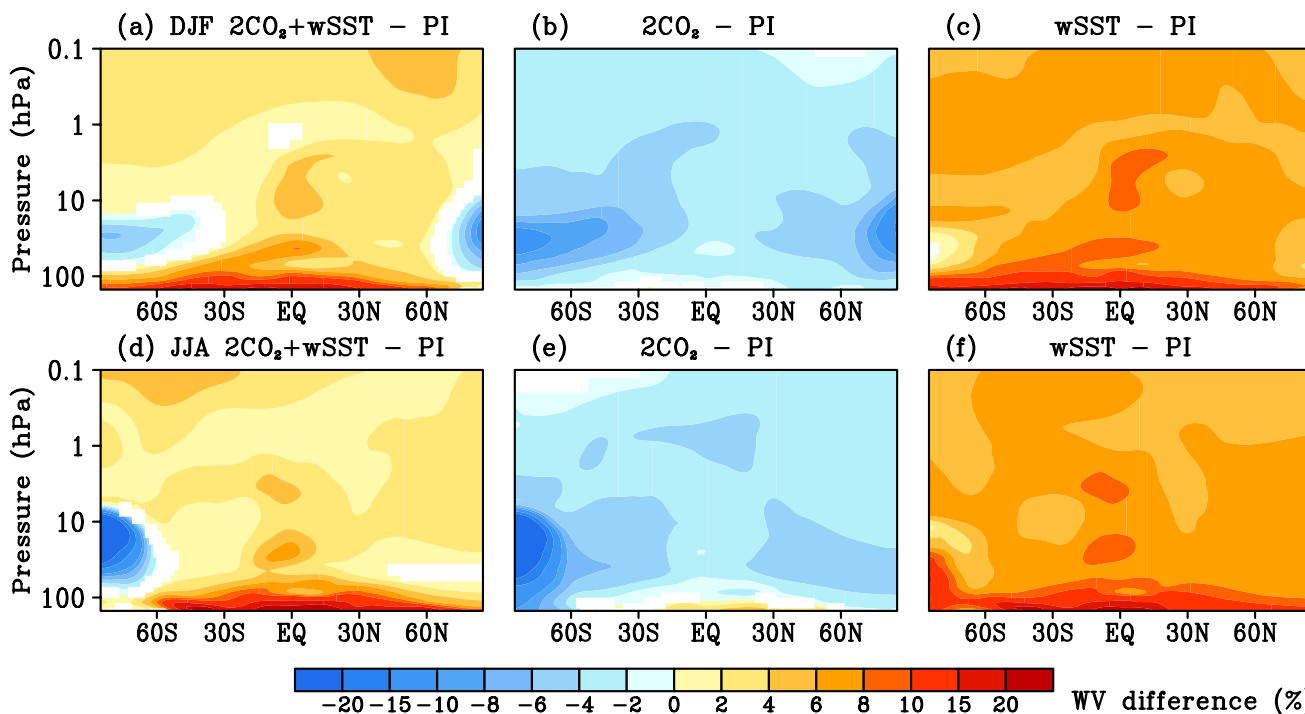


Fig. 3 Comparison of change (from CTL run) in seasonal mean SWV in climate change experiments of CT1 (a, d), C1 (b, e) and T1 (c, f), for DJF means (a–c) and JJA means (d–f). All the shadings are significant at the 5% level

reality, these two effects may not be of equal magnitude and it is likely that changes in stratospheric response are primarily a result of changing the SSTs (Shepherd 2008). The results from WACCM show that the dynamical forcing has larger impact on SWV than the direct radiative forcing. The comparison of the additive response of SWV to CO₂

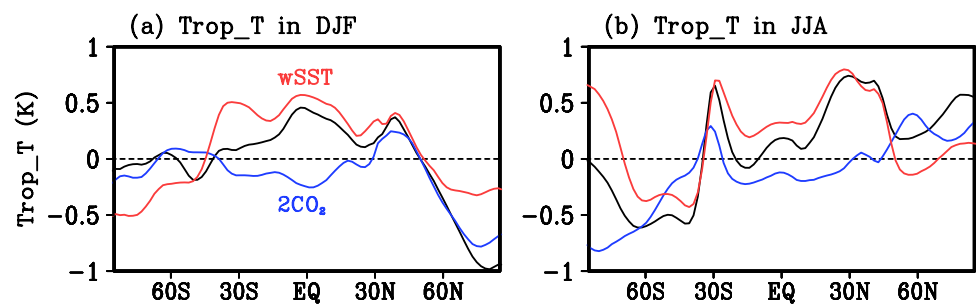
doubling and different warm SSTs patterns is discussed in further detail in Sect. 6.

By examining the SWV response in Fig. 3, we can see that the warm SST effect dominates the change of SWV in most of the stratosphere, except for the two polar regions in the lower stratosphere where the CO₂ doubling induces

a strong decrease in SWV. Previous studies have shown that the lower stratospheric cooling associated with CO₂ doubling may increase the probability of polar stratospheric cloud (PSC) formation (e.g., Pitari et al. 1992). An increase in PSC formation in this area yields a decrease in water vapour, but this is not investigated here. In Fig. 3f, we also observe a large increase in the southern polar lower stratosphere. This polar increase could be associated with the warm stratospheric temperature, which is shown later by the red line in Fig. 4b and the positive difference in Fig. 6f.

The SWV increase is mainly associated with the warm SSTs, which allows for a warmer troposphere and, as a result, leads to a moister troposphere (by the Clausius–Clapeyron relation), and provides a good source for the water vapour entering the stratosphere. The tropical tropopause temperature is highly correlated with the water vapour in the lower stratosphere because of the dehydration resulting from water vapour condensation as the air goes through the tropopause and enters the stratosphere (Fueglistaler et al. 2009; Dessler et al. 2014). Figure 4 shows the changes in the tropopause temperature in three experiments (C1, T1 and CT1). In C1, the tropical and subtropical tropopause is colder than in CTL, which results in less water vapour entering the stratosphere. Therefore, the SST effect on the SWV counteracts the CO₂ effect and lead to more water vapor in the stratosphere. Meanwhile, there is a warmer tropopause from 40° S to 40° N in the experiments T1 and CT1, compared to the PI simulation, which in turn reduces the condensation (dehydration) at the tropopause and allows more water vapour to enter the stratosphere. Consequently, more water vapour is transported upward into the middle and upper stratosphere and poleward to the high-latitudes of both hemispheres through the BDC (Brewer 1949), resulting in more water vapour in the entire stratosphere. It is suggested that the warmer tropopause are due to the weakening of the upwelling in the tropical tropopause, which is affected by the changes of planetary wave activity through the BDC. This is discussed in Sects. 4 and 5.

Fig. 4 Comparison of change (from CTL) in tropopause temperature in climate change experiments of CT1 (black), C1 (blue) and T1 (red), for DJF means (a) and JJA (b) means



4 Response of SWV transport to doubled CO₂ and/or warm SSTs

The residual circulation in the upper stratosphere can be summarized, in short, as being composed of air mass and tracers being transported upward from the summer hemisphere and the tropics to the winter pole where it subsides. Figure 5 shows the changes in the residual circulation along with changes in the vertical velocity w^* in the stratosphere resulting from the experiments CT1, C1 and T1. The significant difference is seen mainly in the upper stratosphere and lower mesosphere around the high-latitudes in the winter hemisphere. In DJF mean (Fig. 5a–c), the upper branch of the circulation that originates in the tropics and subsides in the winter pole is strengthened in all three experiments. The change of w^* in the polar vortex is negative (i.e. stronger subsidence, compared to CTL) in the upper stratosphere and the lower mesosphere, and positive (i.e. weaker subsidence) in the lower stratosphere. These changes in the vertical velocities are accompanied by changes in temperature, which is discussed later. The response in T1 and C1 are of the same sign, and are nearly proportionate, mostly everywhere, with a slightly stronger response of the former.

The changes in JJA mean are comparable to those of DJF mean, but the high-latitude descending branch of the circulation in the winter hemisphere has moved equatorward to 30° S–60° S (Fig. 5d–f). In the polar vortex, there is a positive change of the vertical velocity (rising motion) in the stratosphere and negative (or downwelling) in the mesosphere. In the tropics and subtropics, there is a weak, but significant upwelling change in w^* from the tropopause to the lower stratosphere, which contributes more water vapour to the lower stratosphere.

5 Temperature changes and SWV feedback in the stratosphere

The stratospheric temperature changes in CO₂ doubling scenarios have been investigated using different models and different experimental setups (e.g., Rind et al. 1990, 1998;

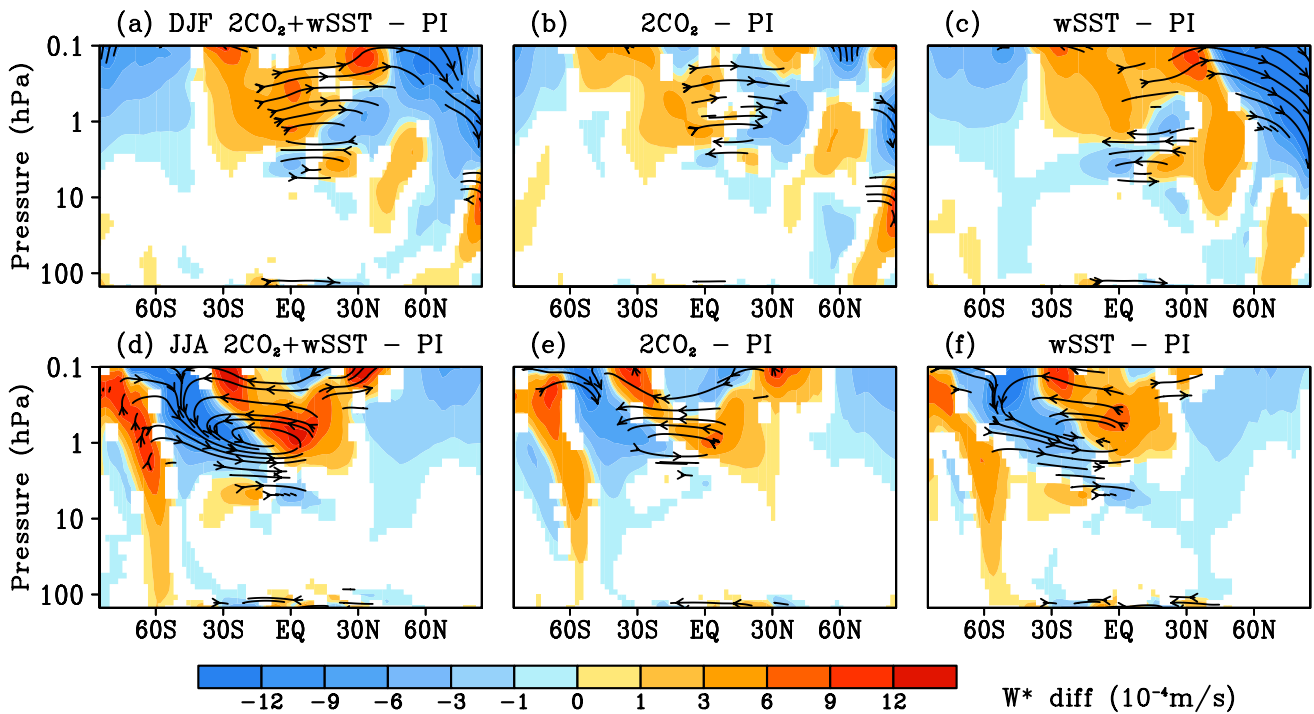


Fig. 5 Comparison of change (from CTL) in residual circulation (stream) and its vertical component w^* (shading) in climate change experiments of CT1 (a, d), C1 (b, e) and T1 (c, f), for DJF means (a–c) and JJA means (d–f). Shown only the 5% significant differences

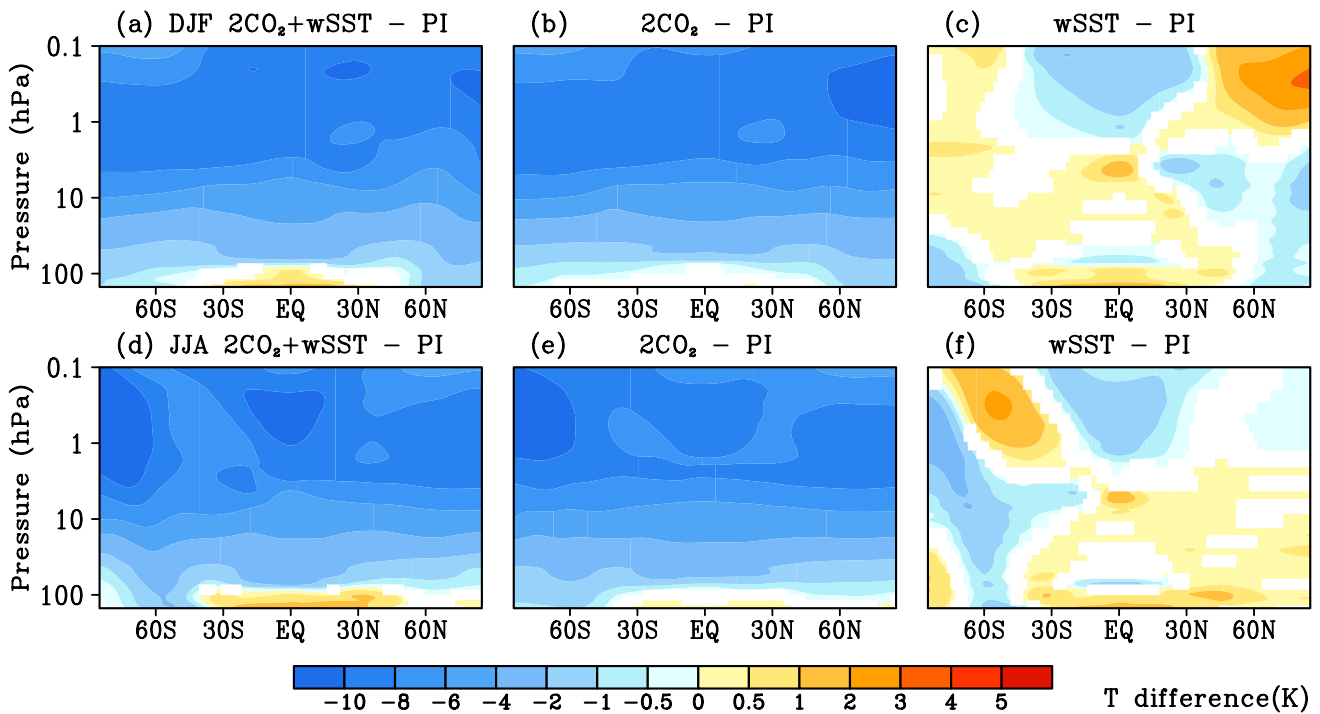


Fig. 6 Comparison of change (from CTL) in seasonal mean stratospheric temperature in climate change experiments of CT1 (a, d), C1 (b, e) and T1 (c, f), for DJF means (a–c) and JJA means (d–f). All the shadings are significant at the 5% level

Langematz et al. 2003; Fomichev et al. 2007). The consensus is that the stratosphere becomes cool in simulations with a doubled CO₂ concentration. There are also indications that the observed stratospheric cooling is not fully caused by in situ effects due to greenhouse gas changes. It is suggested that the observed upper stratospheric temperature trends in low to middle latitudes are caused by radiative effects due to the greenhouse gas changes, while the cooling of the polar stratosphere in winter is enhanced by changes in dynamic heating (Langematz et al. 2003).

Figure 6 shows temperature changes in the stratosphere for the three experiments CT1, C1 and T1. The temperature response of the combined CO₂ doubling with wSST yields general cooling (Fig. 6a, d). The maximum change occurs near the stratopause, with a weak warming in the lower stratosphere. This vertical structure reflects the global-average background temperature distribution, with stronger cooling where temperatures are higher, as expected from radiative arguments, and it is consistent with the previous studies (e.g. Fomichev et al. 2007). Comparing the response to doubled CO₂ and wSST-only, we can observe that the doubled CO₂ (Fig. 6b, e) dominates the combined temperature changes in the stratosphere, except for the tropical lower stratosphere, where a warming anomaly emerges due to warm SSTs (Fig. 6c, f). The impact of doubled CO₂ alone is mainly through radiative-photochemical effect in

the middle atmosphere, as shown by Jonsson et al. (2004), i.e. the temperature changes can be understood primarily as a result of CO₂-induced cooling. The warm SSTs affect the stratosphere strongly in the high-latitude of the winter hemisphere.

As shown in Fig. 6c for the DJF mean with wSST (see Fig. 1), the northern polar region cools in the stratosphere and warms in the lower mesosphere. This pattern of temperature change is mainly associated with the anomaly of upward propagation of planetary waves in northern high-latitude in winter, which often leads to the stratospheric warming anomaly. Figure 7 shows changes in zonal-mean zonal wind and the vertical component of wave activity flux (Eliassen-Palm flux) F_z. The upward propagation of planetary wave in the northern high-latitudes from T1 is weaker than that from CTL run (Fig. 7c), indicating that wSST weakens the warming, which is produced from the planetary wave energy released in the lower stratosphere. The change of zonal-mean zonal wind is positive in the northern pole, indicating a stronger polar vortex. We also observe from Fig. 5c a stronger downwelling in the polar region in the upper stratosphere and lower mesosphere, than that of CTL, which is related to the warming in the lower mesosphere. This downwelling might be formed by wave breaking of stronger gravity waves with easterly wind momentum in the upper mesosphere. In general, anomalous westerlies in the

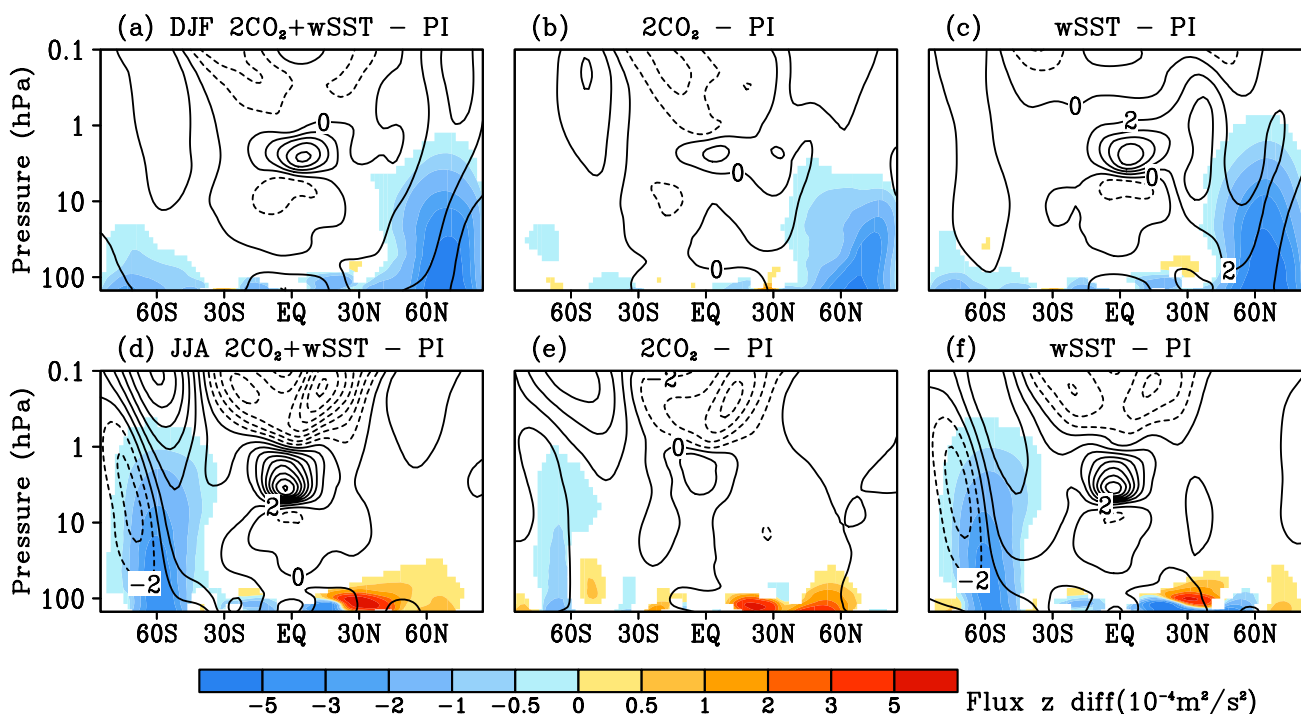


Fig. 7 Comparison of change (from CTL) in zonal mean zonal wind (contour) and vertical wave activity flux F_z (shading) in climate change experiments CT1 (a, d), C1 (b, e) and T1 (c, f), for DJF means (a–c) and JJA means (d–f). All shadings are significant at 5% level

stratosphere (associated with the colder and stronger polar vortex) would enhance vertical propagation of gravity waves (Andrews et al. 1987). Doubling the CO₂-concentration can also induce a weaker upward propagation of the planetary wave activity (Fig. 7b), compared to CTL. However, this reduction is weaker than the reduction resulting from the SST effect.

In austral winter JJA mean, there is a negative change in the upward propagation of the planetary wave activity around 60°S induced by the warm SSTs (Fig. 7f), and a small positive change around 80°S, which explains the temperature changes shown in Fig. 6f, and the polar jet is stronger and moves northward.

How does the wSST affect the planetary wave propagation, which in turn has important repercussions on the temperature of the winter pole? From Fig. 1 we observed a significant cooling in the North Atlantic, which weakens the land-sea thermal contrast in boreal winter, and therefore generates weaker planetary wave activity (Fig. 7c). However, further investigation is needed to clarify whether such a local change of SST could directly influence the large-scale planetary wave activity. Another possible indirect mechanism is that SST changes of North Atlantic would be important for the blocking activity in the Euro-Atlantic sector, which is considered to be intimately associated with the amplification of planetary waves of wave number one (Castanheira and Barriopedro 2010; Martius et al. 2009). In the southern hemisphere (Fig. 7f), the strongest warming in SST is at 60° S, which weakens/enhances the temperature gradient to the north/south of 60° S (much warmer in high-latitude and less warmer in low-latitude and polar region). The changes in temperature gradient could influence the baroclinic wave activity, and changes of the storm track in the troposphere may cause a weaker/stronger upward propagation of wave packets emanating from baroclinic waves and/or blocking events, eventually leading to the weakening/enhancement of planetary wave activity in the southern hemisphere in winter (Castanheira and Barriopedro 2010; Martius et al. 2009).

Another significant and robust temperature change in T1 (Fig. 6c, f) is the warming in the tropical and subtropical lower stratosphere, which dominates the combined response of temperature in CT1 (Fig. 6a, d), whereas there is a non-significant temperature response in this region in C1 (Fig. 6b, e). From Fig. 3 we know that SWV increases greatly in the lower stratosphere in T1 and CT1, which is related to the high tropical and subtropical tropopause temperature. And in turn, as a greenhouse gas, the increased water vapour results in warming in the lower stratosphere, namely, there is a positive feedback between SWV and the temperature in the tropical and subtropical lower stratosphere.

6 Response of SWV to a very warm SSTs scenario

Besides the warm SSTs from first equilibrium stage of Wen et al. (2018), another pattern of warm SSTs, namely wSST2, emerged as an equilibrium response to a doubled CO₂ forcing from the coupled model simulation after a very long time, e.g., 1600 years. This pattern was not obtained and mentioned in other studies, due probably to the fact that the experiments in these studies didn't have a long enough run time. It is reasonable that the very warm SSTs could make a possible future scenario under long time of CO₂ increase. In this response the AMOC recovers and the SST warms everywhere (Fig. 8). The warming in wSST2 is much stronger than those in wSST (Fig. 1), and the strongest change is found along 60° latitude in both hemispheres. As for experiments CT1 and T1, two more experiments, CT2 and T2, are performed with CO₂ doubling and wSST2 combined and separated, respectively.

Figure 9 shows the stratospheric response to wSST2 only. Compared with the response to the wSST discussed in the previous section, the effect of wSST2 on SWV (Fig. 9a, b) is about twice as large (see Fig. 3c, f for T1) in most of the stratosphere, and the maximum, near the tropopause, is more than 20%, suggesting more water vapour comes from the troposphere, and gets transferred to high-latitudes following the residual circulation. The change in residual circulation shows that in DJF mean, the BDC is stronger in the upper stratosphere in lower latitudes in T2 simulations. Unlike T1, the significant change for T2 is in northern high-latitudes. But the significant "warming" change for T2 is in Northern high-latitudes (Fig. 9e), suggesting a stronger downwelling there (although not significant), due to the stronger upward propagation of planetary waves seen

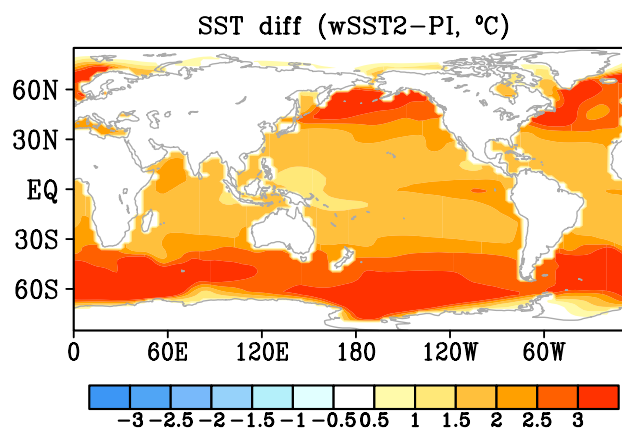


Fig. 8 Annual mean change in sea surface temperature in warm SST2 induced by CO₂ doubling in the coupled CESM compared to the PI SSTs

in Fig. 9g. In JJA mean, the response of the BDC to wSST2 shows that the upper branch from the tropics to the southern hemisphere is enhanced in a very shallow layer, with subsidence around 50° S in the lower mesosphere, merged with an upwelling around 60° S in the upper stratosphere, and followed by an anomalous flow to the tropics around the stratopause. Another significant change occurs around 90° S–60° S where the stream change is opposite to the climatological stream (from north to south). This change inhibits the downwelling or subsidence around 50° S from the lower mesosphere, and yields a water vapour change in the upper stratosphere and lower mesosphere in southern high-latitudes that is not as large as that in the lower stratosphere (less than 10%).

The temperature changes (Fig. 9c–f) show an even stronger positive feedback between temperature and water vapour in the tropical and subtropical stratosphere. In austral winter (Fig. 9f), the temperature response in southern high-latitudes to wSST2 is similar to, but stronger than that in T1 (Fig. 6f). This temperature response pattern can be explained by the fact that in the southern hemisphere, the amplitude of SST in T2 is much stronger than that in T1. The longitudinal gradient is much weaker than that in T1. This decreased gradient weakens the thermal contrast, resulting in an even weaker upward propagation of the planetary wave in the southern high-latitudes (Fig. 9h) than that in T1. This in turn affects the stratospheric temperature in austral winter.

In boreal winter (Fig. 9e), the temperature change in the northern high-latitudes resulting from T2 is opposite to that of T1 (Fig. 6c); there is warming in the stratosphere and cooling in the lower mesosphere. The upward propagation of the planetary waves (Fig. 9g) is stronger than that of CTL, meanwhile the zonal-mean zonal wind in the polar region is easterly anomaly, implying a weaker polar vortex, and these changes are opposite to those of T1 shown in Fig. 7c. This is because in boreal winter, much warmer North Atlantic (and Pacific) in wSST2, with respect to that of PI SSTs, leads to a stronger thermal land-sea contrast in the northern high-latitude. The stronger thermal land-sea contrast could generally enhance baroclinic wave activity, as described previously in Fig. 7. From Fig. 9g, it is clear that the positive anomalies of Fz maximized around 30°N–60°N in the tropopause region are probably due to the enhanced baroclinic wave activity. On the other hand, those seen around 60°N–80°N in the stratosphere are due to the enhanced planetary wave activity, which exist independently from the former. The stratospheric warming in the northern high-latitudes is produced by increasing planetary wave energy in the stratosphere, and results in easterly zonal wind anomaly in the lower stratosphere.

Analysing the SWV response to T1 and T2, we see that the two warm SSTs affect the SWV in the same way, and

the mechanisms seem to be similar. The effect of wSST2 is much stronger because the temperatures of wSST2 are higher. The difference in residual circulation results in a slight difference in the distribution of SWV. Meanwhile, the changes in stratospheric temperature in the northern high-latitudes resulting from these two warm SSTs patterns are opposite. The “warming hole” in the Atlantic induces cooling in the stratosphere and warming in the lower mesosphere, which is opposite to that obtained from wSST2. This difference is explained by the upward propagation of the planetary wave in the winter.

An important issue that arises here is the nature of the interaction between SST and CO₂ doubling in affecting the response. Precisely, we attempt to evaluate this interaction by analysing the linearity of SWV and temperature responses to increasing CO₂ and warm SSTs. We note from the above analysis that the SWV response to CT1 equals the sum of the responses resulting from C1 and T1 separately. As shown in Fig. 10a, b, the difference between the SWV response to CT1 and the sum of responses to C1 and T1 is quite small and not statistically significant in most of the stratosphere. For wSST2 (Fig. 10c, d), however, the difference is significant though small (less than 2% in most of the stratosphere). For temperature change (not shown), similar patterns are obtained for the two warm SSTs, and both show significance in the high-latitude winter, an indication of the (expected) presence of nonlinear processes affecting the stratospheric temperature in high-latitude winter, particularly in the northern polar region, in agreement with Fomichev et al. (2007). The nonlinearity increases when the warm SST getting warmer, both for the response of SWV and stratospheric temperature, which is not shown in previous work with one warm SST scenario.

It is well known that results of numerical experiments depend on parameterizations of physical processes and performance of the used model. The results we present here are consistent with those from other studies using different models. However, in order to overcome the resultant uncertainty, further studies based on multiple climate model intercomparisons should be needed, such as in the CMIP framework, which is left for future research.

7 Summary and conclusions

In this paper, we have used a global high-top atmospheric circulation model WACCM to investigate the response of SWV to a doubling in CO₂ and the dynamic mechanism of the response. To separate the radiative photochemical and dynamical response, sensitivity experiments have

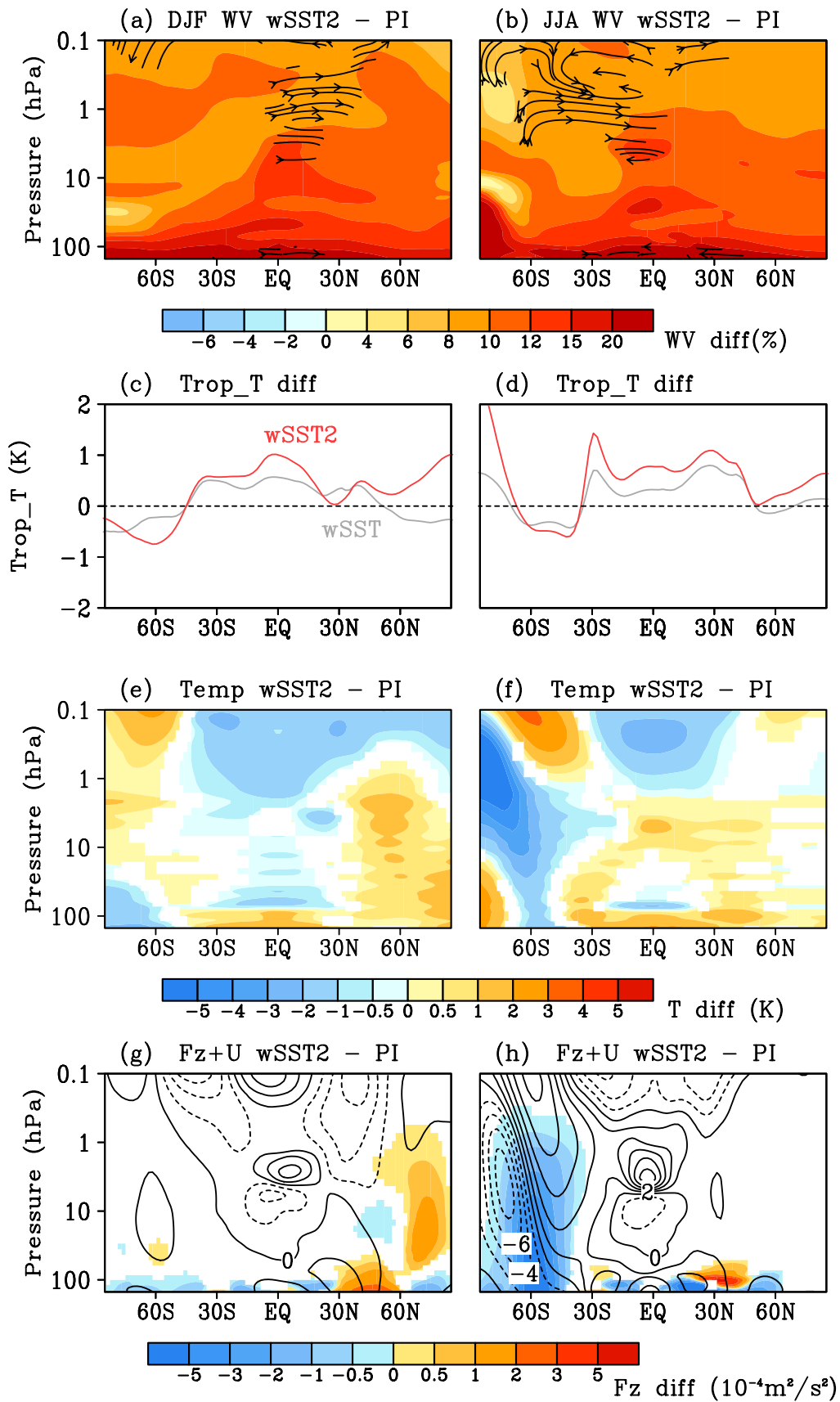


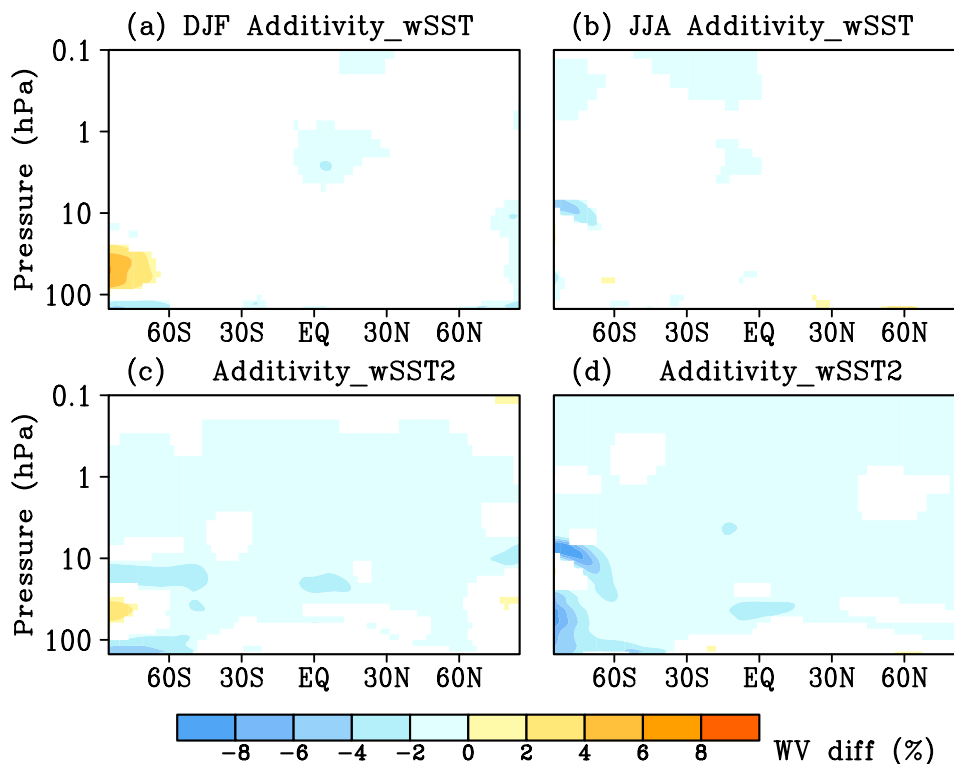
Fig. 9 Stratospheric response to wSST2 (T2): water vapor (shading) and residual circulation (stream) (a, b), tropopause temperature (red line) (c, d), stratospheric temperature (e, f), and zonal-mean zonal wind (contours) and vertical component of the planetary wave activity flux Fz (shading) (g, h) for DJF means (left column) and JJA means (right column). The grey lines in (c, d) are identical to the red lines in Fig. 4 for the experiment T1

been performed by considering changes in CO₂ concentration and corresponding changes in SST combined and separated.

The results show that the warm SSTs result in SWV increase by 6–10% in most of the stratosphere, more than 10% in the lower stratosphere, which dominates the response of SWV to combined changes in most of the stratosphere except the two polar regions in the lower stratosphere, where CO₂-doubling decreases SWV. Some authors (Pitari et al. 1992) suggested that this is because CO₂-doubling increases the probability of PSC formation. The increase of SWV in the lower stratosphere is due to more tropospheric water vapour entering the stratosphere. This can be understood as warm SSTs lead to moister troposphere and a warmer tropopause. The change in the upper branch of the BDC contributes to global water vapour transfer.

The change of atmospheric CO₂ leads to a cooling in most of the stratosphere, except in the tropical and subtropical lower stratosphere, where a warming is seen, which can be attributed to the warmer SSTs. Large increase SWV in the lower stratosphere due to the warm SSTs, which is controlled by tropical tropopause temperature, feedback on temperature in the tropical and subtropical lower stratosphere, reflecting a positive feedback. The effect of warm SSTs on the stratospheric temperature in winter high-latitudes is not strong but still significant. The cold North Atlantic of warm SSTs, due to a reduced AMOC, weakens the upward propagation of planetary waves in boreal winter. This results in a cooling of the lower stratosphere in the high latitudes of the northern hemisphere. However, the warm North Atlantic in wSST2, which strengthens the upward propagation of planetary wave activity in boreal winter, shows the opposite effect with respect to the temperature of northern high-latitudes. Both two warm SSTs affect the southern high-latitudes in austral winter in the same way, i.e. cooling around 60° S in the lower stratosphere, due to the weak SST longitudinal gradient in southern hemisphere resulting in weaker planetary wave activity propagating to the stratosphere.

Fig. 10 Linearity of SWV response to doubled CO₂ and warm SSTs using wSST (a, c) and wSST2 (b, d) for DJF means (a, b) and JJA means (c, d)



Acknowledgements Open access funding provided by Stockholm University. This work is jointly funded by the Swedish National Space Board project Dnr 88/11 “Atmospheric modelling using space-based observations of stable water isotopes” and the Department of Meteorology, Stockholm University. The ERA5 data are downloaded from the ECMWF website. The data analyses are performed on resources provided by the Swedish National Infrastructure for Computing (SNIC) at NSC. Two anonymous reviewers provided constructive comments that helped improve the manuscript.

Open Access This article is licensed under a Creative Commons Attribution 4.0 International License, which permits use, sharing, adaptation, distribution and reproduction in any medium or format, as long as you give appropriate credit to the original author(s) and the source, provide a link to the Creative Commons licence, and indicate if changes were made. The images or other third party material in this article are included in the article’s Creative Commons licence, unless indicated otherwise in a credit line to the material. If material is not included in the article’s Creative Commons licence and your intended use is not permitted by statutory regulation or exceeds the permitted use, you will need to obtain permission directly from the copyright holder. To view a copy of this licence, visit <http://creativecommons.org/licenses/by/4.0/>.

References

- Andrews DG, Holton JR, Leovy CB (1987) Middle atmosphere dynamics (vol 40). Academic Press, Orland, p 489
- Brasseur G, Hitchman MH (1988) Stratospheric response to trace gas perturbations: changes in ozone and temperature distributions. *Science* 240(4852):634–637
- Brewer AW (1949) Evidence for a world circulation provided by the measurements of helium and water vapour distribution in the stratosphere. *Q J R Meteorol Soc* 75(326):351–363
- Caesar L, Rahmstorf S, Robinson A, Feulner G, Saba V (2018) Observed fingerprint of a weakening Atlantic Ocean overturning circulation. *Nature* 556:191–196. <https://doi.org/10.1038/s41586-018-0006-5>
- Castanheira JM, Barriopedro D (2010) Dynamical connection between tropospheric blockings and stratospheric polar vortex. *Geophys Res Lett* 37:L13809. <https://doi.org/10.1029/2010GL043819>
- Dessler AE, Schoeberl MR, Wang T, Davis SM, Rosenlof KH (2013) Stratospheric water vapor feedback. *Proc Natl Acad Sci* 110(45):18087–18091
- Dessler AE, Schoeberl MR, Wang T, Davis SM, Rosenlof KH, Vernier JP (2014) Variations of stratospheric water vapor over the past three decades. *J Geophys Res Atmos* 119(22):12–588
- Drijfhout S, van Oldenborgh GJ, Cimadoribus A (2012) Is a decline of AMOC causing the warming hole above the North Atlantic in observed and modeled warming patterns? *J Clim* 25:8373–8379. <https://doi.org/10.1175/JCLI-D-12-00490.1>
- Fels SB, Mahlman JD, Schwarzkopf MD, Sinclair RW (1980) Stratospheric sensitivity to perturbations in ozone and carbon dioxide: radiative and dynamical response. *J Atmos Sci* 27:2265–2297
- Fomichev VI, Jonsson AI, De Grandpre J, Beagley SR, McLandress C, Semeniuk K, Shepherd TG (2007) Response of the middle atmosphere to CO₂ doubling: results from the Canadian middle atmosphere model. *J Clim* 20(7):1121–1144
- Forster PMDF, Shine KP (1999) Stratospheric water vapour changes as a possible contributor to observed stratospheric cooling. *Geophys Res Lett* 26:3309–3312
- Forster PMDF, Ponater M, Zhong W-Y (2001) Testing broad-band radiation schemes for their ability to calculate the radiative forcing and temperature response to stratospheric water vapour and ozone changes. *Meteorol Z* 10:387–393. <https://doi.org/10.1127/0941-2948/2001/0010-0387>
- Forster PMDF, Shine KP (2002) Assessing the climate impact of trends in stratospheric water vapor. *Geophys Res Lett* 29(6):10–11
- Fueglistaler S, Dessler AE, Dunkerton TJ, Folkins I, Fu Q, Mote PW (2009) Tropical tropopause layer. *Rev Geophys* 47(1)
- Fueglistaler S (2012) Stepwise changes in stratospheric water vapor? *J Geophys Res Atmos* 117(D13)
- Garcia RR, Marsh DR, Kinnison DE, Boville BA, Sassi F (2007) Simulation of secular trends in the middle atmosphere, 1950–2003. *J Geophys Res* 112:D09301. <https://doi.org/10.1029/2006JD007485>
- Gettelman A, Hegglin MI, Son SW, Kim J, Fujiwara M, Birner T, Austin J (2010) Multimodel assessment of the upper troposphere and lower stratosphere: tropics and global trends. *J Geophys Res Atmos* 115(D3)
- Gilford DM, Solomon S, Portmann RW (2016) Radiative impacts of the 2011 abrupt drops in water vapor and ozone in the tropical tropopause layer. *J Clim* 29:595–612. <https://doi.org/10.1175/JCLI-D-15-0167.1>
- Gillett NP, Allen MR, Williams KD (2003) Modelling the atmospheric response to doubled CO₂ and depleted stratospheric ozone using a stratosphere-resolving coupled GCM. *Q J R Meteorol Soc* 129(947–966):2003. <https://doi.org/10.1256/qj.02.102>
- Holton JR, Haynes PH, McIntyre ME, Douglass AR, Rood RB, Pfister L (1995) Stratosphere–troposphere exchange. *Rev Geophys* 33:403–439. <https://doi.org/10.1029/95RG02097>
- Huang Y, Zhang M, Xia Y, Hu Y, Son SW (2016) Is there a stratospheric radiative feedback in global warming simulations? *Clim Dyn* 46(1–2):177–186
- Hurrell JW, Holland MM, Gent PR, Ghan S, Kay JE, Kushner PJ, Lipscomb WH et al (2013) The community Earth system model: a framework for collaborative research. *Bull Am Meteorol Soc*. <https://doi.org/10.1175/BAMS-D-12-00121.1>
- Hurst DF, Oltmans SJ, Vömel H, Rosenlof KH, Davis SM, Ray EA, Jordan AF et al (2011) Stratospheric water vapor trends over Boulder, Colorado: analysis of the 30 year Boulder record. *J Geophys Res Atmos* 116(D2)
- Jahn A, Holland MM (2013) Implications of Arctic sea-ice changes for North Atlantic deep convection and the meridional overturning circulation in CCSM4–CMIP5 simulations. *Geophys Res Lett* 40:1206–1211. <https://doi.org/10.1002/grl.50183>
- Jonsson AI, de Grandpré J, Fomichev VI, McConnell JC, Beagley SR (2004JD) Doubled CO₂-induced cooling in the middle atmosphere: photochemical analysis of the ozone radiative feedback. *J Geophys Res* 109:D24103. <https://doi.org/10.1029/2004JD005093>
- Kim H, An SI (2013) On the subarctic North Atlantic cooling due to global warming. *Theor Appl Climatol* 114:9–19. <https://doi.org/10.1007/s00704-012-0805-9>
- Kinnison DE, Brasseur GP, Walters S, Garcia RR, Marsh DR, Sassi F, Harvey VL, Randall CE et al (2006JD) Sensitivity of chemical tracers to meteorological parameters in the MOZART-3 chemical transport model. *J Geophys Res* 112:D20302. <https://doi.org/10.1029/2006JD007879>
- Langematz U, Kunze M, Krüger K, Labitzke K, Roff GL (2003) Thermal and dynamical changes of the stratosphere since 1979 and their link to ozone and CO₂ changes. *J Geophys Res Atmos* 108(D1):ACL-9
- Lübken F-J, Berger U, Baumgarten G (2013) Temperature trends in the midlatitude summer mesosphere. *J Geophys Res Atmos* 118:13347–13360. <https://doi.org/10.1002/2013JD020576>
- Manabe S, Strickler RF (1964) Thermal equilibrium of the atmosphere with a convective adjustment. *J Atmos Sci* 21(4):361–385

- Manabe S, Wetherald RT (1975) The effects of doubling the CO₂ concentration on the climate of a general circulation model. *J Atmos Sci* 32(1):3–15
- Marsh DR, Mills MJ, Kinnison DE, Lamarque JF, Calvo N, Polvani LM (2013) Climate change from 1850 to 2005 simulated in CESM1 (WACCM). *J Clim* 26:7372–7391. <https://doi.org/10.1175/JCLI-D-12-00558.1>
- Martius O, Polvani LM, Davies HC (2009) Blocking precursors to stratospheric sudden warming events. *Geophys Res Lett* 36:L14806. <https://doi.org/10.1029/2009GL038776>
- Maycock AC, and Shine KP (2012) Stratospheric water vapor and climate: sensitivity to the representation in radiation codes. *J Geophys Res Atmos* 117(D13)
- Maycock AC, Joshi Mm, Shine KP, Scaife AA (2013) The circulation response to idealized changes in stratospheric water vapor. *J Clim* 26(2):545–561
- Neale RB, Richter J, Park S, Lauritzen PH, Vavrus SJ, Rasch PJ, Zhang M (2013) The mean climate of the community atmosphere model (CAM4) in forced SST and fully coupled experiments. *J Clim* 26(14):5150–5168
- Pitari G, Palermi S, Visconti G, Prinn RG (1992) Ozone response to a CO₂ doubling: results from a stratospheric circulation model with heterogeneous chemistry. *J Geophys Res Atmos* 97(D5):5953–5962
- Randel WJ, Wu F, Oltmans SJ, Rosenlof K, Nedoluha GE (2004) Interannual changes of stratospheric water vapor and correlations with tropical tropopause temperatures. *J Atmos Sci* 61(17):2133–2148
- Richter JH, Sassi F, Garcia RR (2010) Toward a physically based gravity wave source parameterization in a general circulation model. *J Atmos Sci* 67(1):136–156
- Rind D, Suozzo R, Balachandran NK, Prather MJ (1990) Climate change and the middle atmosphere. Part I: The doubled CO₂ climate. *J Atmos Sci* 47(4):475–494
- Rind D, Shindell D, Loneragan P, Balachandran NK (1998) Climate change and the middle atmosphere. Part III: The doubled CO₂ climate revisited. *J Clim* 11(5):876–894
- Rind D, Lerner J, Perlwitz J, McLinden C, Prather M (2002) Sensitivity of tracer transports and stratospheric ozone to sea surface temperature patterns in the doubled CO₂ climate. *J Geophys Res Atmos* 107(D24):ACL-25
- Schmidt H, Brasseur GP, Charron M, Manzini E, Giorgetta MA, Diehl T, Walters S (2006) The HAMMONIA chemistry climate model: sensitivity of the mesopause region to the 11-year solar cycle and CO₂ doubling. *J Clim* 19(16):3903–3931
- Sévellec F, Fedorov AV, Liu W (2017) Arctic sea-ice decline weakens the Atlantic meridional overturning circulation. *Nat Clim Change* 7:604–610. <https://doi.org/10.1038/nclimate3353>
- Shepherd TG (2008) Dynamics, stratospheric ozone and climate change. *Atmos Ocean* 46(1):117–138. <https://doi.org/10.3137/ao.460106>
- Sigmond M, Siegmund PC, Manzini E, Kelder H (2004) A simulation of the separate climate effects of middle-atmospheric and tropospheric CO₂ doubling. *J Clim* 17(12):2352–2367
- Smith CA, Haigh JD, Toumi R (2001) Radiative forcing due to trends in stratospheric water vapour. *Geophys Res Lett* 28(1):179–182
- Solomon S, Rosenlof KH, Portmann RW, Daniel JS, Davis SM, Sanford TJ, Plattner GK (2010) Contributions of stratospheric water vapor to decadal changes in the rate of global warming. *Science* 327(5970):1219–1223
- Thornalley DJ, Oppo DW, Ortega P, Robson JJ, Brierley CM, Davis R, Yashayaev I (2018) Anomalously weak Labrador Sea convection and Atlantic overturning during the past 150 years. *Nature* 556(7700):227–230
- Wang T, Zhang Q, Lossow S, Chafik L, Risi C, Murtagh D, Hannachi A (2018) Stable water isotopologues in the stratosphere retrieved from Odin/SMR measurements. *Remote Sens* 10(2):166
- Wen Q, Yao J, Döös K, Yang H (2018) Decoding hosing and heating effects on global temperature and meridional circulations in a warming climate. *J Clim* 31(23):9605–9623. <https://doi.org/10.1175/JCLI-D-18-0297.1>

Publisher's Note Springer Nature remains neutral with regard to jurisdictional claims in published maps and institutional affiliations.